MATERIALS SCIENCE

The alternative Ti-6Al-7Nb alloy has gained extensive progression due to its ability to eliminate the cytotoxicity of vanadium (V) in Ti-6Al-4V alloy for orthopedic implants. The production of titanium alloys by centrifugal casting shows significant potential to reduce costs. Heat treatment and aging can tailor the microstructure and improve the corrosion resistance of titanium alloys. This study examines the effects of various ageing times on the microstructure and corrosion resistance of a centrifugal cast Ti-6Al-7Nb alloy that has previously been heated and treated at a temperature of 1050 °C, and subsequently cooled to room temperature in argon atmosphere gas. Ageing was carried out at a temperature of 550 °C with variable times of 0, 4, 6, and 8 hours. The surface morphology, metal phase changes, and electrochemical characterization were tested using an optical microscope (OM), X-ray diffraction (XRD), potentiodynamic polarization (PDP), and electrochemical impedance spectroscopy (EIS). The basket-weave microstructure is formed where globularization occurs in some phases as ageing time increases. Increasing the FWHM α value is correlated with increasing the amount of α′ martensite phase. As an ageing time enhances, the temperature might offer a greater driving constrain for the nucleation and expansion of the lamellar phase (α). Ageing of 8 hours has the lowest corrosion rate, 0.0023 mpy and highest corrosion resistance, 90457 Ω·cm², due to the partially bimodal structure and grain refinement with a smallest grain size of 327.87 μm. Tafel polarization results show that all passivated samples are stable in the Solution Body Fluid (SBF). This work can be used as a starting point for developing microstructural evolution in titanium alloys

Keywords: orthopedic implant, titanium alloy, ageing time, microstructure, corrosion resistance

UDC 621
DOI: 10.15587/1729-4061.2024.302614

ELECTROCHEMICAL CHARACTERISTIC AND MICROSTRUCTURE OF Ti-6Al-7Nb ALLOY BY CENTRIFUGAL CASTING FOR ORTHOPEDIC IMPLANT BASED ON AGEING TIME VARIATIONS

Anjar Oktikawati
Corresponding author
Postgraduate Student*
E-mail: anjaroktikawati@gmail.com
Rini Riastuti
Profesor of Engineering, Lecturer*
Damisih Damisih
Master of Engineering, Researcher**
I Nyoman Jujur
Doctor of Engineering, Researcher**
Agus Paul Setiawan Kaban
Doctoral student, Researcher
Prof. Johny Wahyuadi Laboratory*
*Department of Metallurgical and Material Engineering
Universitas Indonesia
Kampus Baru UI Depok, Jawa Barat, Indonesia, 16424
**Center of Technology for Material
National Research and Innovation Agency (BRIN)
Puspiptek Area, 224, South Tangerang,
Banten, Indonesia, 15314

Received date 08.02.2024
Accepted date 16.04.2024
Published date 30.04.2024

How to Cite: *Oktikawati, A., Riastuti, R., Damisih, D., Nyoman Jujur, I., Paul Setiawan Kaban, A. (2024). Electrochemical characteristic and microstructure of Ti-6Al-7Nb alloy by centrifugal casting for orthopedic implant based on ageing time variations. Eastern-European Journal of Enterprise Technologies, 2 (12 (128)), 6–15. https://doi.org/10.15587/1729-4061.2024.302614*

1. Introduction

Ti-6Al-7Nb alloy, as a versatile class of α+β titanium alloys, offers attractive properties such as high corrosion and fatigue resistance, biocompatibility, good structural compatibility, and good toughness [1, 2]. It is the most frequently used alternative orthopedic implant material from Ti-6Al-4V that can eliminate the toxicity of vanadium [3, 4]. It also exhibits several functional properties, such as plasticity and high-temperature deformation properties. Solution treatment and ageing are effective processing methods to strengthen the alloy [5, 6].

Centrifugal casting is one option for the low-cost manufacture of orthopedic implants [7]. Numerous researches have shown that residual stress can be reduced and the microstructure of the alloy can be improved by appropriate heat treatment [8, 9]. The microstructure plays an imperative role in the corrosion resistance of the material and can be tailored to improve corrosion resistance. The passive layer's resistance of titanium alloys in the presence of artificial saliva can be enhanced using a heat treatment [10]. The elemental segregation between different phases, which further effectively restricts the formation of the galvanic corrosion, can be obtained by subsequent aging treatment to improve corrosion

resistance. The heat treatment process of titanium alloy significantly influences the microstructure [11]. The previous research [12] studied the effect of heat treatment and ageing at 955 °C/AC/1 h+565 °C/AC/8 h on the microstructure of a TC4 alloy produced by selective laser melting (SLM). The results showed that a basket-weave structure can be obtained after solution with aging treatment, resulting in excellent wear resistance. The outcome from a previous study [13] revealed that a globular microstructure had higher plasticity than a globular microstructure, but lower strength and impact toughness than a lamellar microstructure. Investigation of the effects of aging treatment on the microstructure and the corrosion resistance of laser solid formed (LSFed) Ti-6Al-4V titanium alloy has been carried out. The results revealed that the corrosion resistance of the solution and aging-treated (SATed) Ti-6Al-4 V is slightly better than that of the as-deposited Ti-6Al-4V [14]. It is attributed to the microstructure of the LSFed Ti-6Al-4 V transformed from coarse columnar grains microstructure to more homogeneous basket-weave microstructure after SAT and the β boundary where corrosion occurs preferentially is interrupted or even disappears. Investigation of the grain refinement and mechanical properties of titanium alloy during solution-plus-aging treatment has been carried out. The study reveals that the development of ultra-fine microstructure upon the introduction of severe deformation is shown to significantly improve the corrosion resistance of aging-hardened Cu-3 wt% Ti alloys without sacrificing their mechanical properties [15].

Only a few studies have investigated Ti-6Al-7Nb alloy using the centrifugal casting technique, so the results are not directly available for industrial application. Aging treatment has a significant effect on the secondary phases that precipitate in titanium alloys, resulting in different properties of titanium alloys. Therefore, it is important to study the microstructural evolution of titanium alloys due to their potential applications.

Therefore, a study devoted to aging time which influences microstructural improvement and corrosion resistance of titanium alloys has scientific relevance to the need for orthopedic implants, especially total hip arthroplasty, which is increasing along with the increase in the number of obesity cases due to the sedentarian and another modern human lifestyle. The optimal aging time from as a result of such studies can be applied to similar titanium alloys to obtain the most suitable microstructure for orthopedic implants.

2. Literature review and problem statement

The Ti-6Al-7Nb alloy has received clinical approval and has shown to be a suitable alternative for the Ti-6Al-4V (TC4) alloy, which has been utilized for medical purposes for recent decades [16]. The α+β alloy, Ti-6Al-7Nb, may have its microstructure altered by heating it to a temperature above or below the beta transus (melting point) temperature, T_β, which is an α+β alloy can be engineered using heat treatment and ageing processes with temperatures above or below the beta transus temperature, T_β. These alloys may have their composition, size, and phase distribution altered to some extent. As a consequence, the alloy can be reinforced by heat treatment, ageing, and quenching to get the desired material properties. The mechanical and corrosion characteristics of materials are directly influenced by their microstructure. To produce high strength-ductility matching and enhanced corrosion resistance, the metastable transformation of the $\beta+\Omega\rightarrow\beta+\alpha$ phase can be accomplished by heat treatment. It enables the shift from the sub-stable to the equilibrium phase to achieve excellent strength-ductility matching and improved corrosion resistance [17].

The β transus temperature, T_β, in the Ti-6Al-7Nb alloy is about 1020 °C. Hence, the determined test temperature covers the dual-phase α+β region in the range from 850 °C and 1000 °C and single-phase β in the range of 1050–1150 °C [18]. Sound casting Ti-6Al-7Nb alloy from centrifugal casting technique were reported to be sufficient and conducive for producing very thin parts with complex shapes orthopedic implants because it produces higher castability, fewer cracks, and less porosity than gravity casting [19]. The primary issue regarding the use of titanium and its alloy for orthopedic implants is their low resistance to sliding wear [20]. The low wear resistance of titanium alloy is due to its poor abrasion resistance and undefended oxide layer. Therefore, several surface modification methods have been developed to improve the wear resistance of alloys, such as thermal spray coating which can cause distortion and thermal damage to the substrate if not properly controlled [21], and laser cladding coating because laser cladding equipment is relatively expensive and requires a high level of operator training and experience [22], and chemical composition deposition due to the possibility of collapse under applied stress or sliding velocity, the hard coatings placed on the comparatively soft Ti-6Al-7Nb alloy matrix might be very damaging to their joints implant uses [23]. Furthermore, implementation of such surface modification methods remains difficult due to the compatibility and wettability of the coating within the metal matrix. These problems can be resolved with cost-effective and practical solutions using optimized heat treatment.

The main types of titanium alloy microstructures are lamellar and equiaxed [24]. Lamellar microstructures are formed after slow cooling when heat treatment occurs at a temperature in the single-phase β (β-field) region above T_β, consisting of colonies of lamellar α phase in a β matrix with a diameter of several hundred microns. The equiaxed microstructure is formed after deformation in the two-phase α+β region, i. e. below T_β, composed of a globular α phase dispersed in a β phase matrix. The equiaxed microstructure has a better balance of strength and ductility at room temperature and fatigue properties that are highly dependent on the crystallographic texture of the α hcp phase. In general, fully lamellar titanium alloys have higher fracture toughness and crack resistance, and equiaxed structures have higher cyclic fatigue resistance [25]. A favorable balance of properties can be obtained by the development of a bimodal microstructure consisting of primary α grains and fine lamellar α colonies within relatively small size β grains. Bimodal structures have advantages over other structures in fatigue, ductility, crack growth resistance and creep's properties. Although the qualities of creep resistance and course grain lamellar microstructure are somewhat improved, these microstructures perform poorly in terms of ductility and fatigue. Because of the crystallographic character of the hcp α-phase, the equiaxed globular microstructure shows higher balance of ductility and fatigue. In contrast to course lamellar formations, these features, however, drastically decline at higher temperatures. Therefore, for better balancing of ductility, fatigue, and creep qualities, microstructures with a balance in phase distribution of bimodal structure, where primary α-grains and fine lamellar α+β colonies have been produced [26].

Heat treatment is an effective post-treatment process to optimize microstructure and improve mechanical properties,

with the objectives of which are to reduce residual stresses developed during fabrication, produce the desired combination of material properties, increase strength, and optimize unique properties [27]. In addition, heat treatment plays a vital role in achieving quality characteristics to obtain particular complex technological and/or use characteristics [28].

The α+β alloy can have its microstructure engineered using heat treatment and ageing processes at temperatures above or below T_β. The composition, size and phase distribution of titanium alloys, size and phase distribution of titanium alloys can be manipulated to a certain extent, and then the resulting alloy can be strengthened by heat treatment and cooling, followed by ageing to obtain maximum strength [29]. Heat treatment can improve the microstructure of metal materials and increase mechanical properties.

In addition to improving mechanical properties, heat treatment can also affect the corrosion properties of materials. Microstructure is the main factor that influences the mechanical and corrosion properties of materials. For example, the metastable transformation of the β+Ω→β+α phase can be achieved through heat treatment, which facilitates the transition from the sub-stable to the equilibrium phase to achieve excellent strength-plasticity matching and improved corrosion resistance [30]. Meanwhile, primary α (α_p) and secondary α precipitation (α_s) in titanium alloys are required to achieve perfect strength-plasticity matching and increased corrosion resistance. In addition, coarse columnar grains can be changed to become more homogeneous with solution treatment and aging (STA), thereby increasing the corrosion resistance of the Ti-6Al-4V alloy [31].

The paper [32] showing, that tensile testing and corrosion resistance showed an increase in strength at solution treatment of 1050 °C and aging of 8 hours. However there were unresolved issues related to the microstructure transformation and potentiodynamic polarization which is formed as a result of aging time, the reason for this may be cost part in terms of sample preparation for microstructure observation and polarization test, which makes relevant research impractical. A way to overcome these difficulties can be grinding and polishing to obtain a mirror-like microstructure. This approach was used in [33], however for different titanium alloys. All this suggests that it is advisable to conduct a study on microstructure and potentiodynamic polarization on Ti-6Al-7Nb alloy.

Therefore, the present study endeavored to investigate the influence of ageing treatment on centrifugal casting and heat-treated Ti-6Al-7Nb titanium alloy at 1050 °C, including phase formed, the nature of the microstructure of the alloy, grain size, and corrosion resistance. Corrosion resistance is greatly influenced by the type of microstructure and the grain size. One type of microstructure, namely α+β titanium alloys can be modified to suit the intended application, in this case, to obtain the best combination of mechanical properties and corrosion resistance. All this allows to assert that it is expedient to conduct a study on heat treatment at 1050 °C and ageing time on microstructure and its relationship to corrosion resistance prepared by centrifugal casting of Ti-6Al-7Nb alloy.

3. The aim and objectives of the study

The study aims to unveil the relationship between the ageing time duration of Ti-6Al-7Nb alloy by centrifugal casting to their corrosion resistance under solution body fluid (SBF).

To achieve this aim, the following objectives are accomplished:

– to identify the phase formed of as-cast, heat-treated and aged Ti-6Al-7Nb alloy by centrifugal casting production;

– to determine the nature of the microstructure of the alloy (lamellar, equiaxed, or bimodal);

– to elaborate on the contribution of grain sizes along with the length of ageing time;

– to know how microstructures and grain size modifications affected passive layer development kinetics and anodic behavior, including corrosion resistance and corrosion rate.

4. Material and methods

4. 1. Object and hypothesis of the study

The object of this research is Ti-6Al-7Nb alloy (ASTM F 1295, Daido Steel, Japan). The chemical composition of the material comprises 6.48 Al, 7.13 Nb, 0.24 Fe, 0.01 C, 0.02 N, 0.18 O, 0.01 Ta, 0.01 H, and balance Ti, in mass pct. The Ti-6Al-7Nb alloy with a longer aging time is predicted to have a lower corrosion current density. It is known that low current densities have a low corrosion tendency. In addition, heat treatment and aging have a considerable influence on the secondary α-phase (α_s), the enlargement of the primary α-phase (α_p), grain globularization, and some β phase transformations disappear in titanium alloys which will affect the corrosion resistance of titanium alloys.

4. 2. Centrifugal casting material and method

Centrifugal casting Ti-6Al-7Nb alloy under investigation in this work was formed into a rod. A vacuum electric arc furnace was used to melt wrought Ti-6Al-7Nb rod [31]. A rod was created by casting the molten metals. Ceramic with a zirconium base and nine shell layers make up the casting mold. Argon was employed as a protective environment while melting, pouring, and solidification was carried out in a vacuum centrifugal investment casting machine (Flash Caster, Japan).

4. 3. Heat treatment and ageing

Centrifugal cast Ti-6Al-7Nb alloy was heat treated at temperature β region, i.e. 1050 °C in an argon atmosphere. The heat treatment time was 1 h. Heat-treated at β region to receive Widmänstatten α+β colony structures. Furthermore, the heat-treated samples were aged at 550 °C for 4, 6, and 8 h in an argon atmosphere to decrease desirable residual stresses due to the centrifugal casting process, as well as a decomposition of martensitic α′ to α-phase. They were cooled to room temperature by argon gas flow. The heat treatment process routes are presented in Fig. 1:

– optical microscope (OM).

Metallographic techniques were used to characterize the microstructure of the as-cast, heat-treated (HT), and heat-treated (HT)+ageing. Several mechanical treatments were made, including cutting, mounting, grounding, polishing, engraving, and finishing with alumina paste until a mirror-like surface is obtained, and ensuring that the microstructure is using an optical microscope. These observations were made using an Olympus DSX1000 digital microscope;

– XRD analysis.

An instrumentation tool from Malvern Panalytical's Aeris Benchtop XRD System product line was used to conduct the XRD study. XRD examination was performed on the as-cast, HT, and HT+ageing specimens. The surface was cut, grinding,

and polished to a mirror-like finish. The system operated in the 2θ=5–100° range with Cu Kα anode (1.5406 Å). To improve data acquisition, the samples were rotated while collecting data. The type obtained is simulated to determine the presence of a crystalline phase. Those network parameters and FWHM are processed by Malvern-Panalytical HighScorePlus software;

– corrosion resistance test.

PARSTAT 4000A was used to conduct electrochemical experiments. A typical three-electrode electrochemical cell was employed, with an Ag/AgCl reference electrode and a Pt serving as the counter electrode. As the working electrode to conduct electrochemical experiments, Ti-6Al-7Nb alloy samples were mounted, ground, and polished. Measurements were conducted in simulated body fluid (SBF) for all the tests.

The potential range of –1.2 to 1.5 V vs Ag/AgCl was used to generate potentiodynamic curves of polarization at a scan rate of 0.2 mV/s. Using traces of the polarization profile at 10 mV vs OCP, the resistance of polarization, Rp, was computed.

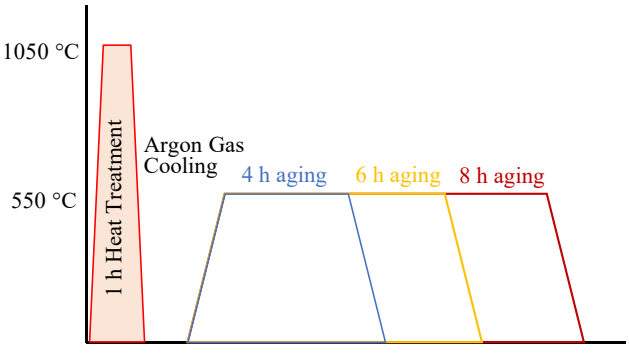

Fig. 1. Schematic overview of the different ageing time conducted – heat treatment at β region (HT), HT+4 h ageing (HTA 4 h), HT+6 h ageing (HTA 6 h), HT+8 h ageing (HTA 8 h)

5. Results of the centrifugal casting for orthopedic implant based on ageing time variations

5. 1. Effect of heat treatment and ageing of Ti-6Al-7Nb alloy on metal phase changes

Fig. 2 shows the XRD profiles of the samples in different conditions: as-cast, heat-treated, and heat-treated+aged samples (4, 6, 8 h). The investigated samples clearly show the presence of similar phases at the same angles of diffraction (2θ), but with different intensities. As-cast, heat-treated (HT), and heat-treated+aged (HTA) samples are mostly α/α′ phase with hexagonal close packed structure (HCP) and β phase with body-centered cubic (bcc) structure.

Table 1 lists the volume and weight fractions of the α(α′) phase with the lowest values obtained for samples that had not been treated at all. After heat treatment there was an increase in the volume fraction and reached the highest value at an ageing time of 8 hours.

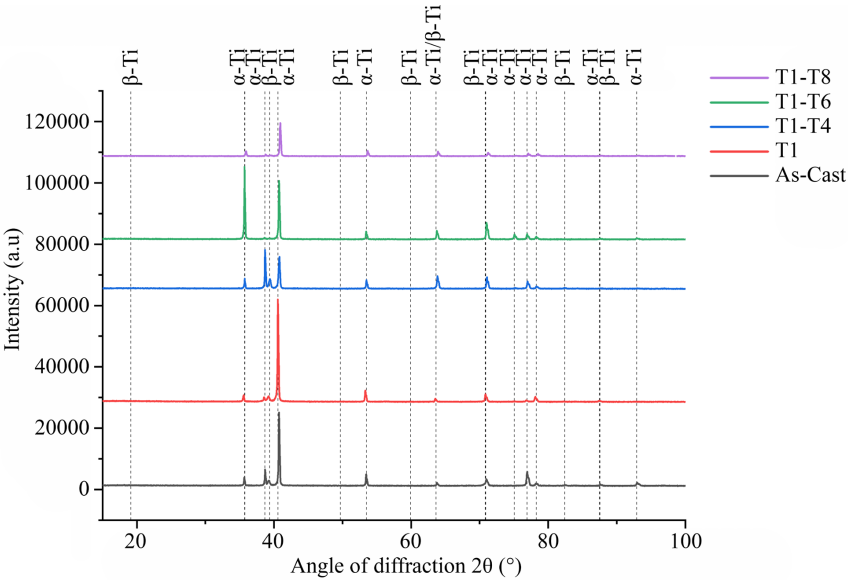

Fig. 2. X-ray diffraction patterns of as-cast and heat treated and aged samples

Table 1

Phase fraction of centrifugal casting Ti-6Al-7Nb alloy

α-Ti Phase	Fraction (%)	
	Volume	Weight
As-cast	88.9665	89
HT	94.2695	94
HT+aging 4 hours	90.9655	91
HT+aging 6 hours	94.4638	94
HT+aging 8 hours	95.3066	95

To distinguish between α- and martensitic α′ phases, the full-width at half-maximum (FWHM) of the three main diffraction peaks of α(α′), namely (101), (002), and (100) are calculated and shown in Table 2.

Table 2

The FWHM of three main diffraction peaks of α/α′ phase

Sample	FWHM		
	(101)	(002)	(100)
As-cast	0.092	0.0881	0.0824
HT	0.0955	0.1094	0.1329
HT+aging 4 hours	0.1352	0.1327	0.1294
HT+aging 6 hours	0.083	0.0771	0.0686
HT+aging 8 hours	0.1487	0.1557	0.1669

As shown in Table 1, the heat-treated sample has a much greater FWHM than the as-cast sample. The FWHM during heat treatment and ageing is listed in Table 2.

5. 2. Microstructure characteristic of Ti-6Al-7Nb alloy

Fig. 3 depicts typical microstructure patterns of alloys with the combination of lamellar α+β (basket-weave microstructure). All of the specimens studied have similar overall microstructural features.

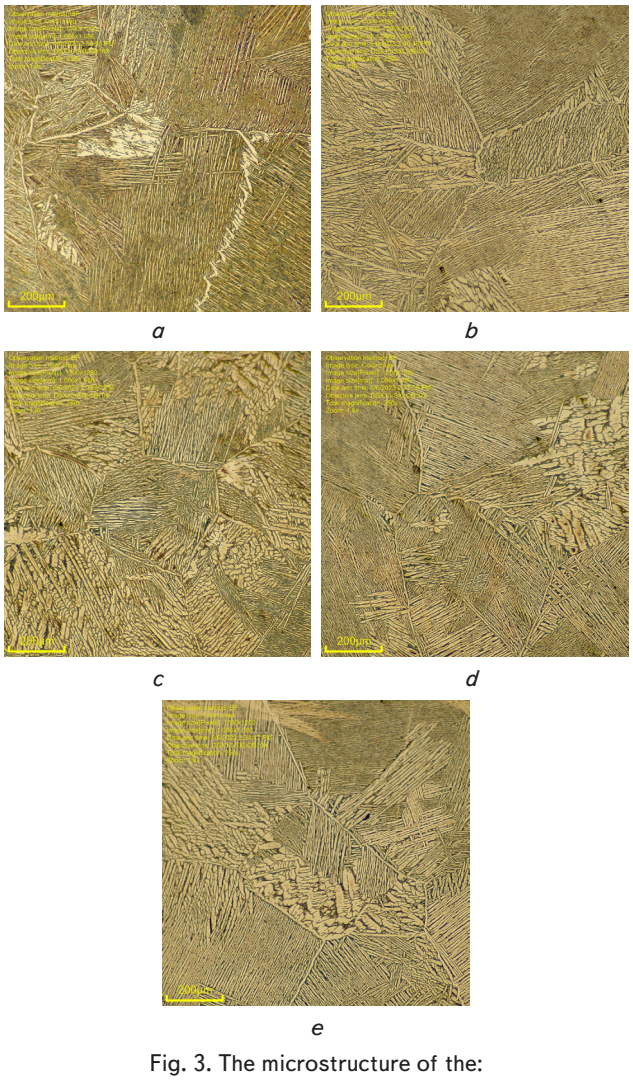

Fig. 3. The microstructure of the: *a* – as-cast Ti-6Al-7Nb alloy; *b* – HT; *c* – HT+4 h ageing; *d* – HT+6 h ageing; *e* – HT+8 h ageing. SEM image showing the α (bright region) and β (dark region) phases

As observed in Fig. 3, the light areas correspond to the α phase, whereas the dark areas belong to the transformed β phase. Heat-treated and aged samples have lamellar shapes that are wider than those seen in as-cast specimens. Fig. 3 demonstrates that as the heat treatment process and ageing period rise, the primary α phase and the grain globularizes steadily increase.

5. 3. Changes in grain size due to heat treatment and ageing

Grain size measurement through observation of the results of an optical microscope (OM) on all Ti-6Al-7Nb alloy samples produced using centrifugal casting techniques aims to determine the homogenization that occurs in the samples after being given heat treatment in the β (T) region = 1050 °C) and different aging times (0, 4, 6, and 8 hours) with a temperature of 550 °C. Table 3 shows quantitative data on the grain size of the Ti-6Al-7Nb alloy based on ASTM E112-13.

Table 3 shows that the smallest grain size was obtained by 8 hours aged sample. Heat treatment and longer aging time make the grain size smaller except for aging during 6 hours.

Table 3

The average grain size of Ti-6Al-7Nb alloy is in accordance with ASTM E112-13

Sample	Grain size average (μm)
As-cast	508.05
HT	485.8
HT+aging 4 hours	473.59
HT+aging 6 hours	698.37
HT+aging 8 hours	327.87

5. 4. Microstructures modifications affected corrosion resistance behavior

Potentiodynamic Polarization (*PDP*).

The potentiodynamic polarization findings of HT and HTA Ti-6Al-7Nb in SBF solution at room temperature are shown in Fig. 4. As-cast specimens are not included because this study wants to know the effect of ageing time variation to the microstructure and characteristic of Ti-6Al-7Nb alloy. The trend of the four cathode polarization curves, as seen in Fig. 4, does not significantly change.

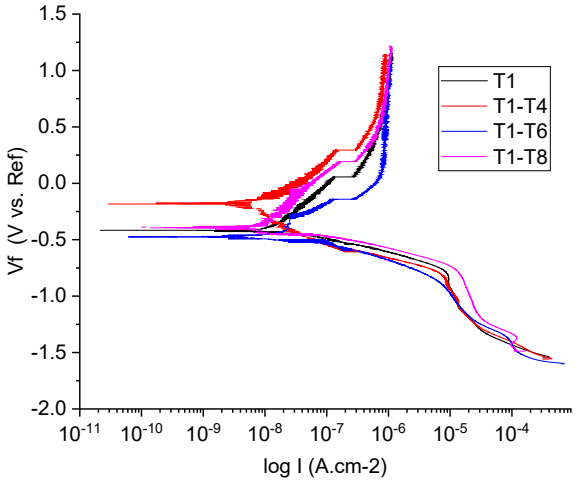

Fig. 4. Potentiodynamic polarization curve Ti-6Al-7Nb centrifugal casting with variations in ageing time

Fig. 4 displays a stable passivation film spreading over a wide potential region with a constant current density over the entire sample. There is no significant difference in the trends of the four cathodic polarization curves, indicating that the same anodic and cathodic reaction occurs on the surface but at different rates. For a better comparison of the polarization behaviour of the specimens in the SBF environment, the confirmed E_{corr} and i_{corr} from Fig. 4 are listed in Table 4.

Table 4

Electrochemical parameters obtained from the Tafel extrapolation method of polarization curve

Sample	E_{corr} (mV)	i_{corr} (nA)	Corrosion rate (mpy)
HT	–416.038	13.180	0.006
HTA 4 h	–175.065	11.916	0.005
HTA 6 h	–469.312	16.047	0.007
HTA 8 h	–387.738	5.3060	0.002

Table 4 lists the results of electrochemical parameters calculated from potentiodynamic polarization curves in SBF solutions. E_{corr} is the corrosion potential whereas i_{corr} is the corrosion current density. It can be seen that the i_{corr} value for HTA 8 hour sample is the lowest compared to other specimens. This shows that the stability of the passive film formed in the HTA 8-hour sample is better compared to other samples to increase performance in corrosion protection. The low corrosion rate is achieved due to the better layer formation and effect caused by the finer grain structure, in accordance with the FWHM value listed in Table 2. The FWHM value, according to the Scherrer equation is inversely proportional to the crystal size [34]. Grain refinement in 8 aging sample is also visible based on the grain size of the microstructure revealed through OM observations.

Electrochemical Impedance Spectroscopy (*EIS*).

The corrosion performance of HT and HTA Ti-6Al-7Nb centrifugal casting alloys was investigated using EIS. The Nyquist plots for HT and HTA Ti-6Al-7Nb were observed, indicating a depressed semicircle, in Fig. 5.

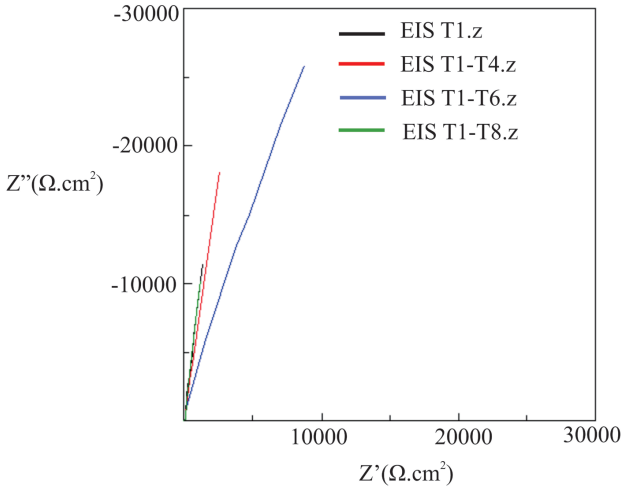

Fig. 5. Nyquist diagram of centrifugal casting Ti-6Al-7Nb alloy with varying ageing times

Fig. 6 shows the equivalent circuit used to fit EIS data and evaluate the corrosion resistance of Ti-6Al-7Nb alloy samples. The impedance response is properly represented using an equivalent circuit that can examine and allow calculation of data relating to the physical and chemical characteristics of the electrochemical process being analyzed. To minimize the effects caused by uneven metal surfaces, a constant phase element (CPE) is introduced into the circuit in pure double-layer capacitance, which provides better fitting.

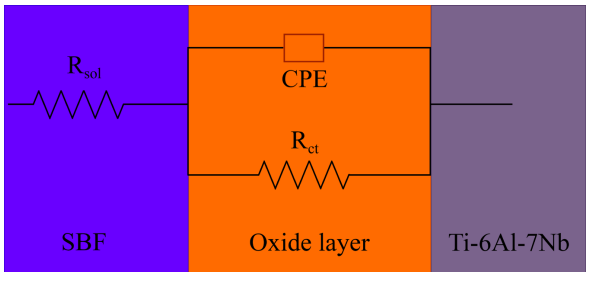

Fig. 6. The electrical circuit used for the fit of experimental data

The values of the EIS parameters, such as R_{ct}, R_{sol} and *CPE*, are represented in Table 5.

Table 5

Electrochemical parameters of equivalent circuits

Sample	R_{sol} (Ω·cm^2)	*CPE* (Ω·cm^2)	R_{ct} (Ω·cm^2)
HT	42.53	1.45×10^{-5}	65883
HTA 4 h	45.72	1.06×10^{-5}	88376
HTA 6 h	46.80	6.18×10^{-6}	46565
HTA 8 h	42.41	1.28×10^{-5}	157120

R_{sol} is the resistance of the electrolyte or solution. The corrosion rate is inversely proportional to the R_{ct} value, and is a function of the movement of electrons across the submerged alloy surface.

6. Discussion of the centrifugal casting for orthopedic implants based on ageing time variations

To discriminate between lamellar (α) and martensitic phase (α′), the FWHM of the third primary α/α′ peaks of diffraction, i. e., (101), (002), and (100) diffraction peak, have been calculated. As shown in Table 1, the heat-treated sample has a much greater FWHM than the as-cast sample, indicating the presence of more martensitic phase (α′) for the HT sample, which results from the transformation generated by furnace cooling throughout the heat treatment process. Furthermore, the FWHM of 8 hours of ageing-treated samples is more significant compared to other specimens, which may be ascribed to the partial α′→α+β evolution [35], exhibiting the declining α′ phases. The martensitic (α′) and lamellar (α) phases coexist after ageing treatment because the martensitic phase (α′) mostly breaks down into the lamellar α-phase and β-phase over ageing treatment. Furthermore, Fig. 3 shows that as ageing time increases, there is a lot of globularization α-phase. It means that the volume percentage of the martensitic phase (α′) decreases, whereas the volume of lamellar α-phase increases (Table 1). It explains by the fact that as an ageing time enhances, the temperature might offer a greater driving constraint for the nucleation and expansion of the lamellar phase (α) during the composition breakdown of the martensitic phase (α′) [35–37].

The FWHM value during heat treatment and ageing is shown in Table 2. In all conditions, there is an increase and decrease in the FWHM value. The lower FWHM values in the as-cast and 6-hour aged samples indicate that these conditions exhibit lower levels of chemical inhomogeneity and internal strain [38].

The gradual cooling from 1050 °C (above the T_β) leads to a combination of lamellar α+β (basket-weave microstructure) develops owing to vacuum gas argon as a cooling medium, similar to the results of previous research [39] that has been comparable findings for the heat-treated temperature's variation and cooling effect's method of Ti-6Al-7Nb alloys achieved comparable findings for the heat-treated and furnace-cooling effect of Ti-6Al-7Nb alloys. Heat-treated and aged (HTA) samples have lamellar shapes that are wider than those seen in as-cast specimens. These colonies are more prominent because the furnace's slow cooling allows for diffusion and growth. Fig. 3 demonstrates that as the heat treatment process and ageing period rise, the primary α phase and

the grain globulars steadily increase, but the volume fraction of α/α′ phase remains unchanged considerably (Table 2). The morphological characteristic of phases changed noticeably; many secondary α phases precipitated in the matrix seemed to merge together and develop, and some β phases disappeared, according to previous study [39–41]. The coarse α phase can be seen in Fig. 3 after being heat-treated and growing in size after ageing (Fig. 3, *b–e*) and cooling with gas argon. When contrasted to the as-cast lath (Fig. 3, *a*), the lamellar begin to coarsen. As a result, when the ageing period rises, the lath gets coarser (Fig. 3, *c–e*). In the Ti-6Al-4V alloy, globularized microstructure, as opposed to martensitic lath, is known to provide excellent strength and toughness. It is widely known that creating a bimodal microstructure in titanium alloy results in an optimal combination of strength and high ductility [42]. A bimodal microstructure with partly equiaxed structures is shown in Fig. 3, *c–e*. Further heat treatment, in this case ageing till eight hours holding time, are required to accelerate lamellar globularization and generate partially equaixed (bimodal) structures. So, among the various treatments in this investigation, it can be considered that 8-hour-aged specimens had the most fantastic deal of optimum balance of excellent ductility and strength.

Furthermore, the heat-treated and aged materials in this study for 8 hours might result in grain refinement (Fig. 3, *e*). Structure refinement might explain the lower rate of corrosion in the 8-hour aged sample. Because tiny grains have more intergranular sites, such as grain boundaries and triple junctions, which are chemically active and have high energy, tiny grains have more intergranular locations, enhanced electron activity, and diffusion-enhanced interaction among the higher energy sites and the electrolyte. Because of the elevated reactivity, there may have been multiple locations for the nucleation of the protective oxide film, leading to the formation of a dense passive film. It is in line with the findings of previous studies [43]. Furthermore, Fig. 3 reveals that the obvious grain boundaries increased with heat treatment and ageing time. The study indicates that improved mechanical adhesion of the oxide layer on the surface is facilitated by a higher density of grain boundaries.

Potentiodinamic Polarization of Heat Treated and Heat Treated+aged Ti-6Al-7Nb Centrifugal Casting Alloy.

The trend of the four cathode polarization curves, as seen in Fig. 5, does not significantly change. It corresponds with the cathodic reaction that takes place on their surfaces at different corrosion rates. Passivation occurred for all samples in the SBF solution. Table 3 lists the E_{corr} and I_{corr} confirmed from Fig. 5 for a better comparison of the polarization behaviour of the HT and HTA Ti-6Al-7Nb alloys. It is seen that the I_{corr} value for the 8-hour aged sample is the lowest among the specimens, indicating that the stability of the passive film generated on the 8-hour aged sample is superior to that of the other specimens. It can also be determined that 8 hours of ageing after 1050 °C heat treatment is more conducive to improving corrosion performance. Low corrosion rates were achieved as a result of the formation and improved layer effect caused by ultrafine grain structures, which coincided with the microstructural features and FWHM value listed in Table 2.

EIS of Heat Treated and Heat Treated+aged Ti-6Al-7Nb Centrifugal Casting Alloy.

The corrosion performance of HT and HTA Ti-6Al-7Nb centrifugal casting alloys was investigated using EIS. The Nyquist plots (Fig. 5) for HT and HTA Ti-6Al-7Nb were observed, indicating a depressed semicircle, as seen in this figure. EIS theory generate that the Nyquist graphs would produce perfect semicircles. The drift from the ideal semicircle was commonly attributed to surface inhomogeneities, resistive mass transfer, and frequency dispersion [44]. Equivalent electric circuits (EEC) for bare metal were employed based on the literature [44–46] to understand the experimental findings, which have been widely used in titanium alloys for medical implants. Fig. 5 shows the equivalent circuit used to fit the EIS data. According to the schematic, solution resistance (R_{sol}) is the electrolyte or solution resistance. The corrosion rate is conversely related to the R_{ct} value, and this is a function of the electron movement across the alloy's submerged surface [47]. The impedance response may be depicted by using electrical circuits that can fit and allow the computation of mathematical information related to the physical and chemical properties of the electrochemical mechanism under inquiry [48]. A constant phase element (*CPE*) was employed in the circuit in place of a pure double-layer capacitance to give a more exact match and reduce the effects brought on by the heterogeneity of the metal surface. The *CPE* described by $Z_{CPE}=1/[Y^0(j\Omega)^n]$, where n is the phase shift's exponent, Ω is the angular frequency, j is the imaginary integer, and Y^0 shows the magnitude of the *CPE*. Depending on the quantity of n, the *CPE* might be a capacitor, inductor, or resistor [49]. Table 4 displays the values of EIS parameters such as *CPE*, R_{sol}, and R_{ct}, demonstrating that R_{ct} values increase in the following order: HTA 8 hour > HTA 4 hour > HT > HTA 6 hour. As the FWHM value increase, so did the thickness of the compact oxide layer.

The limitation of this research is when sample preparation, it would be more representative if the samples were cut before heat treatment and ageing. Moreover if the sample is in the form of an actual implant, for example in the form of a femoral stem. It disadvantages the research concerning the influence of geometry on galvanic corrosion. Furthermore, it may have a slight effect on the microstructure after cutting the post-processed sample even though the wire cut technique is used to cut the sample.

The possible development to address the restriction in the preceding phenomenon is by giving intensive attention to the near-net shape of the cast sample. However, the possible difficulty might be related to how electrochemical impedance spectroscopy (EIS) and potentiodynamic polarization (PDP) testing when the sample has a diameter of less than 25 mm.

Overall, the expected results from the above research can be implemented as a candidate material for orthopedic implants in vitro. Passivation of PDP test results on all samples shows that the centrifugal casting method was successfully applied for the Ti-6Al-7Nb alloy as an orthopedic implant in terms of corrosion resistance. The low rate of corrosion in samples with an aging time of 8 hours shows that the aging time influences the shape of the microstructure and increases corrosion resistance reaching 157120 $\Omega \cdot cm^2$. Moreover, the OM result shows the smallest grain size obtained by 8 aged samples is recovered to achieve maximum protection. The research could be a provision to increase the integrity of orthopedic implant due to the corrosion resistance and lower toxicity in the SBF.

7. Conclusion

1. Revealing the potential of Ti-6Al-7Nb alloy by centrifugal casting as an implant shows that the α+β phase is

formed indicating that this alloy can be modified by heat treatment and aging to obtain the best phase composition to inhibit the corrosion rate of titanium alloys in SBF. Appropriate aging time provides superior volume fraction. This shows an increased volume fraction α after heat treatment and aging for 8 hours.

2. The microstructure observation shows the formation of coarsen α lath (globularization) and finer secondary α. It confirms the bimodal microstructure obtained and increases with the length of ageing time.

3. The FWHM α(α′) increase with the length of aging time in the XRD analysis results, where the pining effect of the primary α which formed during solution treated and aged below β transus, are identified. The FWHM α(α′) is increase to prove that there is a decrease in grain size.

4. The PDP results confirm that the Ti-6Al-7Nb alloy by centrifugal casting both before and after heat treatment and aging shows passivation in the SBF solution. The results of XRD analysis, microstructural observations, and EIS testing are in very good agreement with PDP, where the smaller grain size and the formation of a bimodal structure were identified to increase the corrosion resistance of titanium alloys to SBF solutions.

Conflict of interest

The authors declare that they have no conflict of interest in relation to this research, whether financial, personal, authorship or otherwise, that could affect the research and its results presented in this paper.

Financing

The authors are grateful to Universitas Indonesia for providing funding this research.

Data availability

Manuscript has associated data in a data repository.

Use of artificial intelligence

The authors confirm that they did not use artificial intelligence technologies when creating the current work.

References

1. Davis, J. R. (1998). Metals Handbook Desk Edition. It was prepared under the direction of the ASM International Handbook Committee.
2. Leyens, C., Peters, M. (Eds.) (2003). Titanium and Titanium Alloys. Wiley. https://doi.org/10.1002/3527602119
3. Whittaker, M. (2018). Titanium Alloys 2017. Metals, 8 (5), 319. https://doi.org/10.3390/met8050319
4. Froes, F. H. (2015). TITANIUM Physical Metallurgy Processing and Applications. ASM. Available at: https://www.asminternational.org/wp-content/uploads/files/39989767/39989767-toc.pdf
5. Choubey, A., Balasubramaniam, R., Basu, B. (2004). Effect of replacement of V by Nb and Fe on the electrochemical and corrosion behavior of Ti-6Al-4V in simulated physiological environment. Journal of Alloys and Compounds, 381 (1-2), 288–294. https://doi.org/10.1016/j.jallcom.2004.03.096
6. Tamilselvi, S., Raman, V., Rajendran, N. (2006). Corrosion behaviour of Ti-6Al-7Nb and Ti-6Al-4V ELI alloys in the simulated body fluid solution by electrochemical impedance spectroscopy. Electrochimica Acta, 52 (3), 839–846. https://doi.org/10.1016/j.electacta.2006.06.018
7. Ndukwe, A. I. (2022). Review of Recent Findings on Investment Casting of Titanium Alloys. Academic Journal of Manufacturing Engineering, 20 (2), 99–108. Available at: https://www.ajme.ro/PDF_AJME_2022_2/L12.pdf
8. Su, B., Luo, L., Wang, B., Su, Y., Wang, L., Ritchie, R. O. et al. (2021). Annealed microstructure dependent corrosion behavior of Ti-6Al-3Nb-2Zr-1Mo alloy. Journal of Materials Science & Technology, 62, 234–248. https://doi.org/10.1016/j.jmst.2020.05.058
9. Gu, B., Chekhonin, P., Xin, S. W., Liu, G. Q., Ma, C. L., Zhou, L., Skrotzki, W. (2021). Microstructure and texture development during hot-compression of Ti5321. Materials Characterization, 179, 111297. https://doi.org/10.1016/j.matchar.2021.111297
10. Hulka, I., Florido-Suarez, N. R., Mirza-Rosca, J. C., Saceleanu, A. (2022). Mechanical Properties and Corrosion Behavior of Thermally Treated Ti-6Al-7Nb Dental Alloy. Materials, 15 (11), 3813. https://doi.org/10.3390/ma15113813
11. Lei, L., Zhao, Y., Zhao, Q., Wu, C., Huang, S., Jia, W., Zeng, W. (2021). Impact toughness and deformation modes of Ti-6Al-4V alloy with different microstructures. Materials Science and Engineering: A, 801, 140411. https://doi.org/10.1016/j.msea.2020.140411
12. Yao, L., He, Y., Wang, Z., Peng, B., Li, G., Liu, Y. (2021). Effect of Heat Treatment on the Wear Properties of Selective Laser Melted Ti-6Al-4V Alloy Under Different Loads. Acta Metallurgica Sinica (English Letters), 35 (3), 517–525. https://doi.org/10.1007/s40195-021-01280-8
13. Tian, Y., Li, S., Hao, Y., Yang, R. (2013). High temperature deformation behavior and microstructure evolution mechanism transformation in Ti2448 alloy. Acta Metallurgica Sinica, 48 (7), 837–844. https://doi.org/10.3724/sp.j.1037.2012.00007
14. Wang, G., Zhao, Z., Yu, B., Chen, Z., Wang, Q., Yang, R. (2017). Effect of Heat Treatment Process on Microstructure and Mechanical Properties of Titanium Alloy Ti6246. Chinese Journal of Materials Research, 31 (5), 352–358. https://doi.org/10.11901/1005.3093.2016.621
15. Lee, C. S., Kim, M. G., Kim, G.-H., Kim, K.-T., Hwang, D., Kim, H. S. (2019). Corrosion Properties of Ultra-Fine-Grained Cu-3 wt % Ti Alloy Fabricated by Combination of Hot Rolling and Aging Treatment. Journal of Nanoscience and Nanotechnology, 19 (10), 6487–6492. https://doi.org/10.1166/jnn.2019.17071
16. Avinash, D., Leo Kumar, S. P. (2021). Investigations on surface-integrity and mechanical properties of biocompatible grade Ti-6Al-7Nb alloy. Materials Technology, 37 (9), 897–905. https://doi.org/10.1080/10667857.2021.1903671

17. Gao, K., Zhang, Y., Yi, J., Dong, F., Chen, P. (2024). Overview of Surface Modification Techniques for Titanium Alloys in Modern Material Science: A Comprehensive Analysis. Coatings, 14 (1), 148. https://doi.org/10.3390/coatings14010148
18. Yang, X., Dong, X., Li, W., Feng, W., Xu, Y. (2020). Effect of solution and aging treatments on corrosion performance of laser solid formed Ti-6Al-4V alloy in a 3.5 wt. % NaCl solution. Journal of Materials Research and Technology, 9 (2), 1559–1568. https://doi.org/10.1016/j.jmrt.2019.11.082
19. Senopati, G., Rahman Rashid, R. A., Kartika, I., Palanisamy, S. (2023). Recent Development of Low-Cost β-Ti Alloys for Biomedical Applications: A Review. Metals, 13 (2), 194. https://doi.org/10.3390/met13020194
20. Li, X. X., Zhou, Y., Ji, X. L., Li, Y. X., Wang, S. Q. (2015). Effects of sliding velocity on tribo-oxides and wear behavior of Ti-6Al-4V alloy. Tribology International, 91, 228–234. https://doi.org/10.1016/j.triboint.2015.02.009
21. Khun, N. W., Tan, A. W. Y., Bi, K. J. W., Liu, E. (2016). Effects of working gas on wear and corrosion resistances of cold sprayed Ti-6Al-4V coatings. Surface and Coatings Technology, 302, 1–12. https://doi.org/10.1016/j.surfcoat.2016.05.052
22. Weng, F., Yu, H., Chen, C., Liu, J., Zhao, L., Dai, J., Zhao, Z. (2017). Effect of process parameters on the microstructure evolution and wear property of the laser cladding coatings on Ti-6Al-4V alloy. Journal of Alloys and Compounds, 692, 989–996. https://doi.org/10.1016/j.jallcom.2016.09.071
23. Marenych, O. O., Ding, D., Pan, Z., Kostryzhev, A. G., Li, H., van Duin, S. (2018). Effect of chemical composition on microstructure, strength and wear resistance of wire deposited Ni-Cu alloys. Additive Manufacturing, 24, 30–36. https://doi.org/10.1016/j.addma.2018.08.003
24. Sieniawski, J., Ziaja, W., Kubiak, K., Motyk, M. (2013). Microstructure and Mechanical Properties of High Strength Two-Phase Titanium Alloys. Titanium Alloys - Advances in Properties Control. https://doi.org/10.5772/56197
25. Guan, S., Solberg, K., Wan, D., Berto, F., Welo, T., Yue, T. M., Chan, K. C. (2019). Formation of fully equiaxed grain microstructure in additively manufactured AlCoCrFeNiTi0.5 high entropy alloy. Materials & Design, 184, 108202. https://doi.org/10.1016/j.matdes.2019.108202
26. Yan, C., Hao, L., Hussein, A., Young, P. (2015). Ti-6Al-4V triply periodic minimal surface structures for bone implants fabricated via selective laser melting. Journal of the Mechanical Behavior of Biomedical Materials, 51, 61–73. https://doi.org/10.1016/j.jmbbm.2015.06.024
27. Matthew, J., Donachie, M. (2001). Heat treating titanium and its alloys. HEAT TREATIN G PRO G RESS. Available at: https://www.academia.edu/32143147/Titanium_A_Technical_Guide
28. Bălţatu, M. S., Vizureanu, P., Bălan, T., Lohan, M., Ţugui, C. A. (2018). Preliminary Tests for Ti-Mo-Zr-Ta Alloys as Potential Biomaterials. IOP Conference Series: Materials Science and Engineering, 374, 012023. https://doi.org/10.1088/1757-899x/374/1/012023
29. Semiatin, S. L. (2020). An Overview of the Thermomechanical Processing of α/β Titanium Alloys: Current Status and Future Research Opportunities. Metallurgical and Materials Transactions A, 51 (6), 2593–2625. https://doi.org/10.1007/s11661-020-05625-3
30. Zuo, H., Deng, H., Zhou, L., Qiu, W., Xu, P., Wei, Y. et al. (2022). The effect of heat treatment on corrosion behavior of selective laser melted Ti-5Al-5Mo-5V-3Cr-1Zr alloy. Surface and Coatings Technology, 445, 128743. https://doi.org/10.1016/j.surfcoat.2022.128743
31. Seo, S., Park, J. (2023). Annealing Heat Treatment for Homogenizing the Microstructure and Mechanical Properties of Electron-Beam-Welded Thick Plate of Ti-6Al-4V Alloy. Materials, 16 (23), 7423. https://doi.org/10.3390/ma16237423
32. Winda Sari, M. (2019). Studi pengaruh temperatur solution treatment dan waktu aging terhadap sifat mekanik serta ketahanan korosi pada paduan implan biomedis Ti-6Al-7Nb hasil centrifugal casting. S1 thesis, Universitas Sultan Ageng Tirtayasa. Available at: https://eprints.untirta.ac.id/6046/
33. Yang, Z., Li, J., Zhang, B., Li, J. (2022). Microstructures and mechanical properties of a titanium alloy thick plate joint after electron beam welding plus solution-aging. Journal of Materials Research and Technology, 19, 913–922. https://doi.org/10.1016/j.jmrt.2022.05.091
34. Muniz, F. T. L., Miranda, M. A. R., Morilla dos Santos, C., Sasaki, J. M. (2016). The Scherrer equation and the dynamical theory of X-ray diffraction. Acta Crystallographica Section A Foundations and Advances, 72 (3), 385–390. https://doi.org/10.1107/s205327331600365x
35. Su, B., Wang, B., Luo, L., Wang, L., Liu, C., Su, Y. et al. (2022). Tuning microstructure and improving the corrosion resistance of a Ti-6Al-3Nb-2Zr-1Mo alloy via solution and aging treatments. Corrosion Science, 208, 110694. https://doi.org/10.1016/j.corsci.2022.110694
36. Liang, Z., Sun, Z., Zhang, W., Wu, S., Chang, H. (2019). The effect of heat treatment on microstructure evolution and tensile properties of selective laser melted Ti6Al4V alloy. Journal of Alloys and Compounds, 782, 1041–1048. https://doi.org/10.1016/j.jallcom.2018.12.051
37. Xu, W., Brandt, M., Sun, S., Elambasseril, J., Liu, Q., Latham, K. et al. (2015). Additive manufacturing of strong and ductile Ti-6Al-4V by selective laser melting via in situ martensite decomposition. Acta Materialia, 85, 74–84. https://doi.org/10.1016/j.actamat.2014.11.028
38. Chanfreau, N., Poquillon, D., Stark, A., Maawad, E., Mareau, C., Dehmas, M. (2022). Phase transformation of the Ti-5553 titanium alloy subjected to rapid heating. Journal of Materials Science, 57 (9), 5620–5633. https://doi.org/10.1007/s10853-022-06959-6
39. Xu, C., Sikan, F., Atabay, S. E., Muñiz-Lerma, J. A., Sanchez-Mata, O., Wang, X., Brochu, M. (2020). Microstructure and mechanical behavior of as-built and heat-treated Ti–6Al–7Nb produced by laser powder bed fusion. Materials Science and Engineering: A, 793, 139978. https://doi.org/10.1016/j.msea.2020.139978

40. Yu, J., Yin, Z., Huang, Z., Zhao, S., Huang, H., Yu, K. et al. (2022). Effect of Aging Treatment on Microstructural Evolution and Mechanical Properties of the Electron Beam Cold Hearth Melting Ti-6Al-4V Alloy. Materials, 15 (20), 7122. https://doi.org/10.3390/ma15207122
41. Lei, Z., Chen, Y., Ma, S., Zhou, H., Liu, J., Wang, X. (2020). Influence of aging heat treatment on microstructure and tensile properties of laser oscillating welded TB8 titanium alloy joints. Materials Science and Engineering: A, 797, 140083. https://doi.org/10.1016/j.msea.2020.140083
42. Li, C.-L., Hong, J.-K., Narayana, P. L., Choi, S.-W., Lee, S. W., Park, C. H. et al. (2021). Realizing superior ductility of selective laser melted Ti-6Al-4V through a multi-step heat treatment. Materials Science and Engineering: A, 799, 140367. https://doi.org/10.1016/j.msea.2020.140367
43. Mahadule, D., Khatirkar, R. K., Gupta, S. K., Gupta, A., Dandekar, T. R. (2022). Microstructure evolution and corrosion behaviour of a high Mo containing α+β titanium alloy for biomedical applications. Journal of Alloys and Compounds, 912, 165240. https://doi.org/10.1016/j.jallcom.2022.165240
44. Scully, J., Silverman, D., Kendig, M. (Eds.) (1993). Electrochemical Impedance: Analysis and Interpretation. ASTM International. https://doi.org/10.1520/stp1188-eb
45. Stępień, M., Handzlik, P., Fitzner, K. (2016). Electrochemical synthesis of oxide nanotubes on Ti6Al7Nb alloy and their interaction with the simulated body fluid. Journal of Solid State Electrochemistry, 20 (10), 2651–2661. https://doi.org/10.1007/s10008-016-3258-8
46. Li, B. Q., Xie, R. Z., Lu, X. (2020). Microstructure, mechanical property and corrosion behavior of porous Ti–Ta–Nb–Zr. Bioactive Materials, 5 (3), 564–568. https://doi.org/10.1016/j.bioactmat.2020.04.014
47. Mansfeld, F. (1990). Electrochemical impedance spectroscopy (EIS) as a new tool for investigating methods of corrosion protection. Electrochimica Acta, 35 (10), 1533–1544. https://doi.org/10.1016/0013-4686(90)80007-b
48. Boukamp, B. (1986). A Nonlinear Least Squares Fit procedure for analysis of immittance data of electrochemical systems. Solid State Ionics, 20 (1), 31–44. https://doi.org/10.1016/0167-2738(86)90031-7
49. Ibriş, N., Mirza Rosca, J. C. (2002). EIS study of Ti and its alloys in biological media. Journal of Electroanalytical Chemistry, 526 (1-2), 53–62. https://doi.org/10.1016/s0022-0728(02)00814-8